17. Franceschetti, A., Fu, H., Wang, L. W. & Zunger, A. Many-body pseudopotential theory of excitons in InP and CdSe QDs. *Phys. Rev. B.* (in the press).
18. Leung, K., Pokrant, S. & Whaley, K. B. Exciton fine structure in CdSe nanoclusters. *Phys. Rev. B* **57,** 12291–12301 (1998).
19. Kovalev, E. *et al.* Optically induced polarization anisotropy in porous Si. *Phys. Rev. Lett.* **77,** 2089–2092 (1996).
20. Bruchez, M. Jr *et al.* Semiconductor nanocrystals as fluorescent biological labels. *Science* **281,** 2013–2016 (1998).
21. Chan, C. W. & Nie, S. Quantum dot bioconjugates for ultrasensitive nonisotopic detection. *Science* **381,** 2016–2018 (1998).
22. Hines, M. A. & Guyot Sionnest, P. Synthesis and characterization of strongly luminescing ZnS-capped CdSe nanocrystals. *J. Phys. Chem.* **100,** 468–471 (1996).
23. Dabbousi, B. O. *et al.* (CdSe)ZnS core-shell quantum dots: synthesis and characterization of a size series of highly luminescent nanocrystallites. *J. Phys. Chem. B* **101,** 9463–9475 (1997).
24. Fattinger, C. & Lukosz, W. Optical-environment-dependent lifetimes and radiation patterns of luminescent centers in very thin films. *J. Lumin.* **31&32,** 933–935 (1984).

Acknowledgements. We thank A. P. Efros for discussions. S.A.E. thanks the Lester Wolfe Foundation and Eastman Chemical Co. for fellowships. This work was funded in part by the NSF-MRSEC program and the AT&T Foundation. We thank the M.I.T. Harrison Spectroscopy laboratory for support and for use of its facilities.

Correspondence and requests for materials should be addressed to M.G.B. (e-mail: mgb@mit.edu).

Size and form in efficient transportation networks

Jayanth R. Banavar*, Amos Maritan† & Andrea Rinaldo‡

* *Department of Physics and Center for Materials Physics, 104 Davey Laboratory, The Pennsylvania State University, University Park, Pennsylvania 16802, USA*
† *International School for Advanced Studies (SISSA), Via Beirut 2–4, 34014 Trieste, and INFM and the Abdus Salam International Center for Theoretical Physics, 34014 Trieste, Italy*
‡ *Ralph M. Parsons Laboratory, Department of Civil and Environmental Engineering, Massachusetts Institute of Technology, Cambridge, Massachusetts 02139, USA, and Dipartimento di Ingegneria Idraulica, Marittima e Geotecnica, Università di Padova, Padova, Italy*

Many biological processes, from cellular metabolism to population dynamics, are characterized by allometric scaling (power-law) relationships between size and rate[1–10]. An outstanding question is whether typical allometric scaling relationships—the power-law dependence of a biological rate on body mass—can be understood by considering the general features of branching networks serving a particular volume. Distributed networks in nature stem from the need for effective connectivity[11], and occur both in biological systems such as cardiovascular and respiratory networks[1–8] and plant vascular and root systems[1,9,10], and in inanimate systems such as the drainage network of river basins[12]. Here we derive a general relationship between size and flow rates in arbitrary networks with local connectivity. Our theory accounts in a general way for the quarter-power allometric scaling of living organisms[1–10], recently derived[8] under specific assumptions for particular network geometries. It also predicts scaling relations applicable to all efficient transportation networks, which we verify from observational data on the river drainage basins. Allometric scaling is therefore shown to originate from the general features of networks irrespective of dynamical or geometric assumptions.

In euclidean geometry, a D-dimensional compact object, characterized by a linear size L and having a constant density (independent of L), has a volume V and a mass M that scale as L^D. Thus, simple geometrical attributes that depend on L should scale with the mass as a function of $M^{1/D}$. For example, the surface area of such objects scales as $M^{(D-1)/D}$. For three-dimensional objects (where $D = 3$), one may therefore expect scaling to hold with the exponents being related to the factor 1/3. But we will show here that, for systems comprising transportation networks, this simple $1/D$-scaling is no longer valid.

To model the metabolic system of living organisms, we postulate that the fundamental processes of nutrient transfer at the microscopic level are independent of organism size. In a D-dimensional organism (denoted the service region), the number of such transfer sites scales as L^D (here L is measured in units of l, the mean distance between neighbouring sites). Each transfer site is fed with nutrients (for example, through blood) by a central source through a network providing a route for the transport of the nutrients to the sites. The total amount of nutrients being delivered to the sites per unit time, B, simply scales as the number of sites or as L^D. The total blood volume C for a given organism at any given time depends, in the steady-state supply situation, on the structure of the transportation network. It is proportional to the sum of individual flow rates in the links or bonds that constitute the network. We define the most efficient class of networks as that for which C is as small as possible. Note that this does not coincide with the assumption made in ref. 8, where the energy dissipation was minimized within a hierarchical model.

Our key result is that, for networks in this efficient class, C scales as $L^{(D+1)}$. The total blood volume increases faster than the metabolic rate B as the characteristic size scale of the organism increases. Thus larger organisms have a lower number of transfer sites (and hence B) per unit blood volume. Because the organism mass scales[1–3,5–7] (at least) as C, the metabolic rate does not scale linearly with mass, but rather scales as $M^{D/(D+1)}$. In the non-biological context, the number of transfer sites is proportional to the volume of the service region, which, in turn, leads to a novel mass–volume relationship.

We consider a single network source that services L^D sites uniformly distributed in a D-dimensional space. Each site is connected to one or more of its neighbours, which results in a transportation network that spans the system. Such a network may be a well connected one with loops, or merely a spanning tree, an extreme example of which is a spiral structure[11] (Fig. 1a–d). Each site X is supplied by the source at a steady rate F_X, no less than a positive value $F_{\min}$ and no larger than a value $F_{\max}(F_{\max} \geq F_{\min})$, both of which may depend on l. A simple, special case would correspond to a uniform constant rate for all sites. We set $l = 1$ without loss of generality. Such a system could represent a biological organism that needs a steady supply of nutrients to all its parts[1–8]. The metabolic rate of such a biological organism is given by $B = \Sigma_X F_X$ and simply scales as L^D. Another example is the (inverse) problem of the drainage basin of a river where the sites represent source areas, F_X is the net rainfall rate of landscape-forming events[12] and the network provides routes for transport of water and sediments.

Any transportation network must provide a route from the source to all the L^D sites and consists of interconnected links in each of which, in steady state, the flow rate does not change with time. Each link starts or terminates at the source or a site. Let the scalar quantity $|I_b|$ represent the magnitude of the flow on the b-th link. The source has an outward flow, whose rate exactly equals the sum of the flow rates into all the sites. At a junction of the links, a conservation law for the net flow holds—the inflow must exactly balance the outflow plus the amount supplied to the site. This conservation law does not determine uniquely the flow on each link for an arbitrary network. The degrees of freedom in the choice of the flow pattern is controlled by the number of independent loops equal to (the number of links) − (the number of sites) + 1. The total quantity of nutrients in the network at any instant of time, C, is given simply by $\Sigma_b|I_b|$ on setting the constant of proportionality equal to 1.

We propose the theorem that for any spanning network in D dimensions, C scales at least as L^{D+1} and at most as L^{2D} for large L. Equivalently, the number of transfer sites or B scales at most as $C^{D/(D+1)}$ and at least as $C^{1/2}$. The general proof of the theorem is presented as Supplementary Information. A simple argument is that C is equal to the number of transfer sites (L^D) multiplied by the mean distance of the transfer sites to the source (the father away a transfer site is from the source as measured along the network, the larger the amount of blood that will be needed to nourish it). This

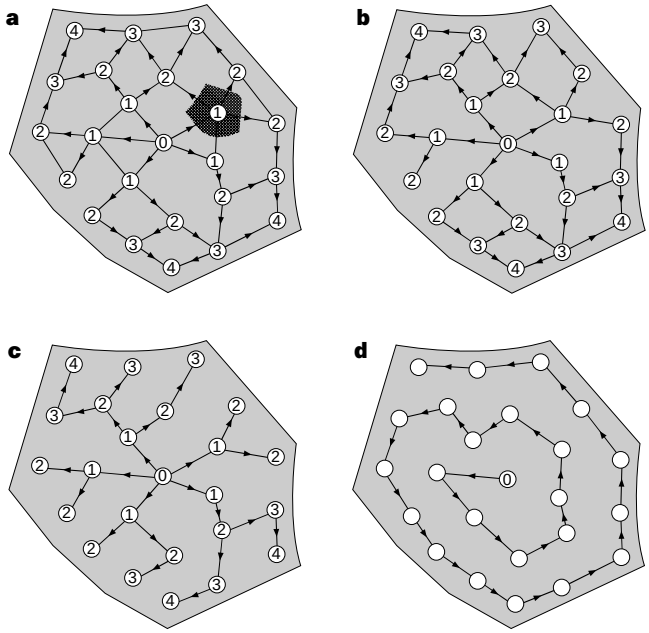

Figure 1 Sketches of transportation networks. **a**, An example of a fully connected network, defined as the connection pattern of links that join the sites, generically denoted by X, characterized by different distances L_X from the source O. The node number in the drawing represents the value of L_X defined to be the minimum number of sites encountered among all the routes along the network from O to X. The cross-hatched area represents the elementary service volume V_X of one of the sites. Each site X may be thought of as serving an elementary volume V_X requiring the necessary nutrient supply F_X. Two sites are defined as neighbours if their service volumes share a part of their boundaries of non-zero measure. The arrows denote orientated links that are directed away from the source. **b**, Maximal directed network. Only orientated links are retained from the fully connected network. **c**, A directed spanning tree. Each site is connected to the source by a single path, the shortest, belonging to the maximal network. **d**, A spiral pattern, which yields limiting scaling behaviour. Note that within the assumed framework of local connectivity, the possibility of explosion patterns[11] connecting all sites directly to the source is not admissible.

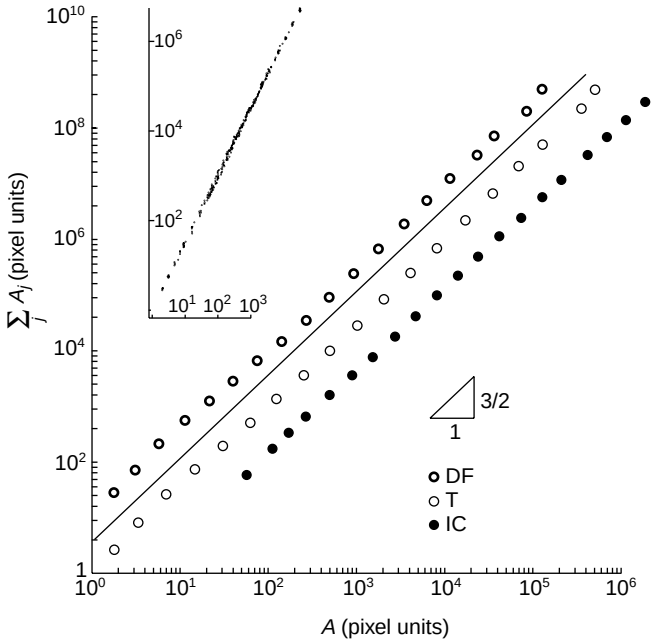

Figure 2 Allometric scaling in river networks. Double logarithmic plot of $C \propto \Sigma_{X\in\gamma}A_X$ versus A for three river networks characterized by different climates, geology and geographic locations (Dry Fork, West Virginia, 586 km^2, digital terrain map (DTM) size 30 × 30 m^2; Island Creek, Idaho, 260 km^2, DTM size 30 × 30 m^2; Tirso, Italy, 2,024 km^2, DTM size 237 × 237 m^2). The experimental points are obtained by binning total contributing areas, and computing the ensemble average of the sum of the inner areas for each sub-basin within the binned interval. The figure uses pixel units in which the smallest area element is assigned a unit value. Also plotted is the predicted scaling relationship with slope 3/2. The inset shows the raw data from the Tirso basin before any binning has been done.

mean distance scales at least as L and at most as L^D. The latter result holds for a network with a one-dimensional topology as in a space-filling spiral, whereas the former result is obtained when the network has all links directed away from the source (or towards a collection point or the outlet in the river basin). Indeed, C scales as L^{D+1} for all directed networks (the flow in all but the links of the directed maximal network (Fig. 1b) are necessarily zero in these cases) independent of whether they have loops or a tree-like structure, provided I_b is non-negative on each link. Such solutions do indeed exist and include all directed trees (Fig. 1c). These solutions belong to the class of the most efficient networks in that they lead to the smallest value of C. In such networks, B scales as $C^{D/(D+1)}$. Thus, for $D = 3$, when quantities related to the network are scaled with respect to C, we obtain quarter-power scaling rather than the one-third power behaviour discussed earlier.

The application of our theorem to the problem of allometric scaling in living organisms, which span size scales that range over many orders of magnitude[1–8], is straightforward. In spite of an impressive array of scales and the accompanying diverse requirements in the resources needed for sustaining the organism, a robust and common feature is that a variety of biological quantities (generically denoted as Y) that are related to blood circulation scale algebraically with the mass M of the organism. The relation is given as $Y \sim M^s$, where s is a scaling exponent[1–8]. Even though the organisms are three-dimensional, the exponent s is usually consistently found to be obtained from the fraction 1/4.

West, Brown and Enquist[8] have constructed a model of space-filling hierarchical networks of branching tubes to explain allometric scaling. In our analysis, the mass M of an organism scales as the blood volume C, so that in the simplest and most efficient scenario $B \sim M^{3/4}$, which is the central result of allometric scaling[1–10]. Many of the other exponents derived in ref. 8 follow from simple dimensional analysis, thus accounting for their robustness, whereas others depend on detailed assumptions. The scaling exponent is universal. Our analysis shows that the basic result does not require any assumptions regarding the hierarchical nature of the network nor does it necessarily demand a tree-like structure. However, the presence of a tree would greatly shorten the total length of the network, thereby increasing its viability and efficiency. Observed differences in scaling within a species and between species[1–7] could arise from factors extrinsic to the network that limit the amount of nutrients delivered to the sites (see Supplementary Information).

We now turn to a test of the theorem within the context of river networks[12]. An elevation map of the soil heights of the rugged landscape may be used to derive a spanning tree that defines unique routes from each location within the basin to the global outlet, where the main stream is formed. Suitably accurate data and objective procedures to extract the network are known, and the reliability of the observational results are well established[12]. Each site X in the basin is associated with a sub-basin that drains into it. The role of the metabolic rate for this sub-basin is taken by the total contributing area, which is defined by the recursion relation $A_X = \Sigma_{Z\in nn(X)}A_Z + 1$, where $nn(X)$ are the nearest neighbours of X that drain into X through appropriate steepest-descent drainage directions. Note that the added unity is the area of the elementary pixel, the analogue of F_X. Indeed, if A is the area of the sub-basin that drains into a given site X, the analogue of C is defined by $\Sigma_{Z\in\gamma}A_Z$

where γ is the collection of all sites connected to X through drainage directions. The theorem predicts that, for efficient drainage basins, a log–log plot of C versus A should have a slope of 3/2 because $D = 2$ and river networks in nature are known to be efficient and directed[12]. Our observational data (Fig. 2) are found to agree with the predictions over five decades of scales.

Our general results should be applicable to a wide variety of distributed networks including the flow of water, blood, sewage, food, air and electrical currents. Even though the specific details vary significantly, the novel behaviour built into efficient transportation networks provides a unified framework[13] underlying the allometric scaling of diverse systems. □

Received 17 August 1998; accepted 10 March 1999.

1. McMahon, T. A. & Bonner, J. T. *On Size and Life* (Scientific American Library, New York, 1983).
2. Bonner, J. T. *The Evolution of Complexity by Means of Natural Selection* (Princeton Univ. Press, Princeton, 1983).
3. Peters, R. H. *The Ecological Implications of Body Size* (Cambridge Univ. Press, Cambridge, 1983).
4. Feldman, H. A. & McMahon, T. A. The 3/4 mass exponent for energy metabolism is not an artifact. *Respir. Physiol.* **52,** 149–163 (1983).
5. Schmidt, Nielsen, K. *Scaling: Why is Animal Size so Important?* (Cambridge Univ. Press, Cambridge, 1984).
6. Calder, W. A. III *Size, Function and Life History* (Harvard Univ. Press, Cambridge, Massachusetts, 1984).
7. Brown, J. H. *Macroecology* (Univ. Chicago Press, Chicago, 1995).
8. West, G. B., Brown, J. H. & Enquist, B. J. A general model for the origin of allometric scaling laws in biology. *Science* **276,** 122–126 (1997).
9. Enquist, B. J., Brown, J. H. & West, G. B. Allometric scaling of plant energetics and population density. *Nature* **395,** 163–165 (1998).
10. Damuth, J. D. Common rules for animals and plants. *Nature* **395,** 115–116 (1998).
11. Stevens, P. S. *Patterns in Nature* (Little, Brown, Boston, 1974).
12. Rodriguez-Iturbe, I. & Rinaldo, A. *Fractal River Basins: Chance and Self-Organization* (Cambridge Univ. Press, New York, 1997).
13. Wilson, E. O. *Consilience: The Unity of Knowledge* (Knopf, New York, 1997).

Supplementary information is available on *Nature*'s World-Wide Web site (http://www.nature.com) or as paper copy from the London editorial office of *Nature*.

Acknowledgements. We thank R. Rigon for the computations shown in Fig. 2; A. Beauvais, F. Colaiori, P. Dodds, A. Flammini, M. Caterina Putti, R. Robinett, I. Rodriguez-Iturbe, D. Rothman and J. Weitz for helpful discussions; and John Damuth for many key insights. This work was supported by INFN, NASA, NATO, MURST 40% *Trasporto di sedimenti ed evoluzione morfologica di corsi d'acqua, estuari e lagune alle diverse scale temporali* and The Donors of the Petroleum Research Fund administered by the American Chemical Society.

Correspondence and requests for materials should be addressed to J.R.B. (e-mail: jayanth@phys.psu.edu).

Electronic mechanism of hardness enhancement in transition-metal carbonitrides

Seung-Hoon Jhi*, Jisoon Ihm*, Steven G. Louie† & Marvin L. Cohen†

** Department of Physics and Center for Theoretical Physics, Seoul National University, Seoul 151-742, Korea*
† Department of Physics, University of California at Berkeley, Berkeley, California 94720–7300, USA and Materials Science Division, Lawrence Berkeley National Laboratory, Berkeley, California 94720, USA

Transition-metal carbides and nitrides are hard materials widely used for cutting tools and wear-resistant coatings. Their hardness is not yet understood at a fundamental level. A clue may lie in the puzzling fact that transition-metal carbonitrides that have the rock-salt structure (such as TiC_xN_{1-x}) have the greatest hardness for a valence-electron concentration of about 8.4 per cell[1–3], which suggests that the hardness may be determined more by the nature of the bonding than by the conventional microstructural features that determine the hardness of structural metals and alloys. To investigate this possibility, we have evaluated the shear modulus of various transition-metal carbides and nitrides using *ab initio* pseudopotential calculations. Our results show that the behaviour of these materials can be understood on a fundamental level in terms of their electronic band structure. The unusual hardness originates from a particular band of σ bonding states between the non-metal *p* orbitals and the metal *d* orbitals that strongly resists shearing strain or shape change. Filling of these states is completed at a valence-electron concentration of about 8.4, and any additional electrons would go into a higher band which is unstable against shear deformations.

Among the various microscopic and intrinsic properties of materials, the shear modulus provides a measure of the rigidity against the shape deformations involved in microhardness indentation experiments. In particular, since the Peierls stresses in the transition-metal carbonitrides are very high, the strengths of these compounds may be influenced more by the difficulty of nucleating and moving dislocations through the background crystal lattice than by the difficulty of moving dislocations through microstructural obstacles[4]. As the stresses required to nucleate or move isolated dislocations scale with the shear modulus, electronic changes that affect the shear modulus may have a pronounced effect on the macroscopic hardness value. Several prior discussions of the mechanical properties of hard materials have made this point[4–8]. There is more than one shear modulus, but we have elected to study c_{44} (rather than, say, the difference between c_{11} and c_{12} or averaged shear modulus) which by itself represents a shape change without volume change, and provides directly information about electronic response to shear strain.

To understand the variation of the shear modulus c_{44} with composition, we carried out quantum-mechanical electronic-structure calculations (under both normal and strained conditions) for TiC_xN_{1-x}, HfC_xN_{1-x} and $Zr_xNb_{1-x}C$ using the *ab initio* pseudopotential method[9,10]. In our calculations, alloy configurations such as TiC_xN_{1-x} are simulated in two different ways and cross-checked. The first is the virtual crystal method in which the ionic pseudopotential

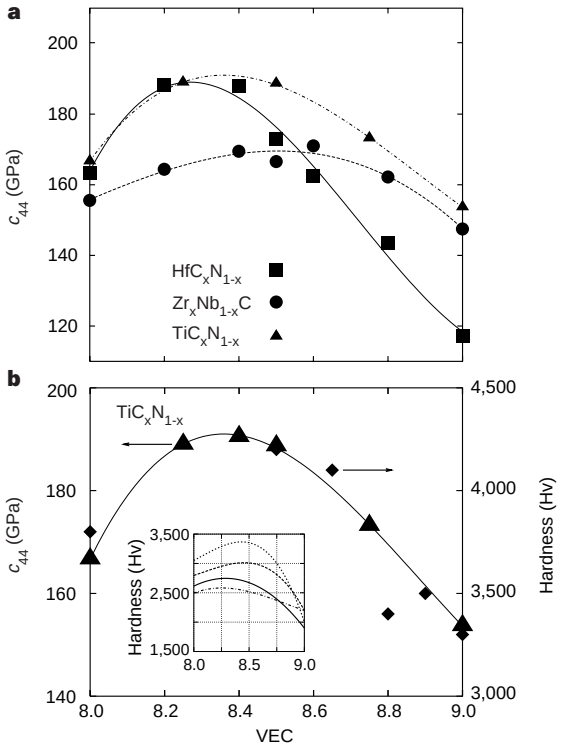

Figure 1 Correlation between the calculated shear modulus c_{44} and experimental microhardness. **a**, Calculated shear modulus c_{44} in GPa for TiC_xN_{1-x} (filled triangles), HfC_xN_{1-x} (filled boxes) and $Zr_xNb_{1-x}C$ (filled circles) as a function of the valence electron concentration (VEC). The curves are polynomial fits to the calculated c_{44}. **b**, Measured microhardness of TiC_xN_{1-x} cermets from ref. 2 in Hv units (filled diamonds). For comparison, the calculated c_{44} (filled triangles) in GPa is plotted in the same figure. The thin solid line is a guide to the eye. Inset, microhardness of bulk alloys and sub-stoichiometric compounds (Ti(CN), dotted line; (ZrNb)C, dashed line; Hf(CN), solid line; and NbC_{1-x}, dash-dotted line).